

**Slope Stability and Lateral Earth Force Interslice  
Functions Based on Finite Analysis**

**By**

**Harianto Rahardjo, Lecturer  
Nanyang Technological Institute  
Singapore 2263**

**and**

**Delwyn G. Fredlund, Professor  
Department of Civil Engineering  
University of Saskatchewan  
Saskatoon, SK Canada S7N 0W0**

**and**

**Ken K. Fan, Geotechnical Engineer  
98 - 410 Koauka Loop  
21 - A AIEA  
Hawaii, USA 96701**

**Presented to  
CSCE Specialty Conference on  
Stability and Performance of Slopes and Embankments-II  
University of California at Berkeley  
June 29 - July 1, 1992**

## Slope Stability and Lateral Earth Force Interslice Functions Based on Finite Element Analysis

Hariato Rahardjo<sup>1</sup>, Delwyn G. Fredlund<sup>2</sup>, M. ASCE, and Ken K. Fan<sup>3</sup>

### ABSTRACT

The indeterminacy of limit equilibrium method of slices is commonly resolved by using an assumption regarding the interslice forces. An appropriate interslice force function can be predicted using a finite element stress analyses. A bell-shaped function was found to represent the interslice force function for slope stability problems. For active lateral earth force problems, a stress analysis showed that the interslice force function was essentially triangular in shape. For passive lateral earth force problems, a high shear stress was observed in the proximity of the wall, which rapidly diminished to zero at some distance behind the wall.

### INTRODUCTION

Limit equilibrium methods of slices have commonly been used to analyze the stability of slopes. The same principles of limit equilibrium can also be applied to the lateral earth force analyses (Janbu, 1957; and Morgenstern and Eisenstein, 1970). Complete equilibrium is satisfied through force and moment equilibriums. However, these statical equilibrium equations together with the Mohr-Coulomb failure criterion are insufficient to render the problem determinate. The problem of indeterminacy is commonly solved by making an assumption regarding the direction of the interslice forces (Fredlund, Krahn and Pufahl, 1981).

For slope stability analyses, the calculated factors of safety does not vary significantly with different interslice force assumptions (Bishop, 1955). On the other hand, unreasonable assumptions may cause difficulties in obtaining a convergent solution for the nonlinear factors of safety equations.

---

<sup>1</sup> Lecturer, Nanyang Technological Institute, Singapore 2263

<sup>2</sup> Professor, Department of Civil Engineering, University of Saskatchewan, Saskatoon, SK Canada S7N 0W0

<sup>3</sup> Geotechnical Engineer, 98, 410 Koauka Loop, 21 - A AIEA, Hawaii USA 96701

In the calculation for lateral earth force, the selection of the interslice force assumption has a greater effect for the passive case than for the active case (Rowe, 1963 and Rahardjo, 1982). Various assumptions for the interslice force direction have been found to result in significantly different passive earth forces. As a result, it is important to use an appropriate assumption of interslice forces when performing limit equilibrium analyses.

### INTERSLICE FUNCTIONS IN METHODS OF SLICES

The direction of the interslice forces in a soil mass can be described by relating the interslice shear forces to the interslice normal forces in any vertical plane through use of a mathematical function of the following form (Morgenstern and Price, 1965) (Fig. 1).

$$\frac{X}{E} = \lambda f(x) \quad [1]$$

where:

$X$  = interslice shear force

$E$  = interslice normal force

$f(x)$  = a functional relationship which describes the manner in which the magnitude of  $X/E$  varies across the slip surface

$\lambda$  = a scaling constant which represents the percentage of the function,  $f(x)$ , used in the analysis

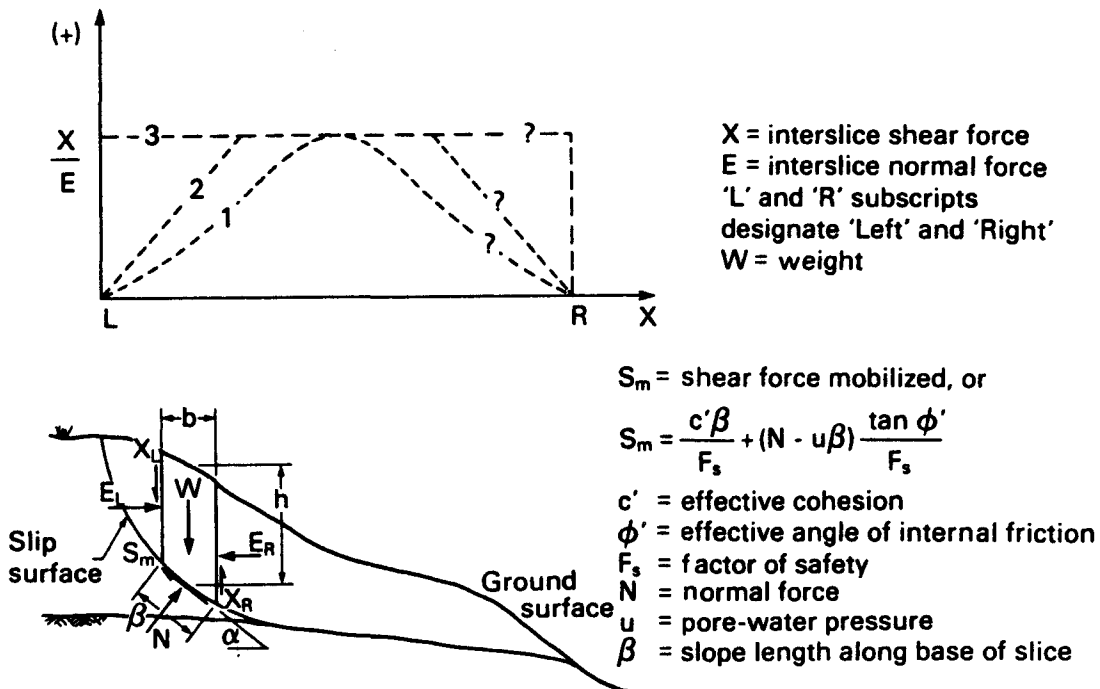


Fig. 1 Assumed interslice force functions for slope stability

Several possible interslice force functions,  $f(x)$ , that can be assumed for slope stability and lateral earth force problems are illustrated in Figs. 1 and 2, respectively. The suitability of each function must be examined in order to achieve a "physically acceptable" solution (Morgenstern and Price, 1965). Consequently, the position of the computed line of thrust should fall within the potential sliding mass.

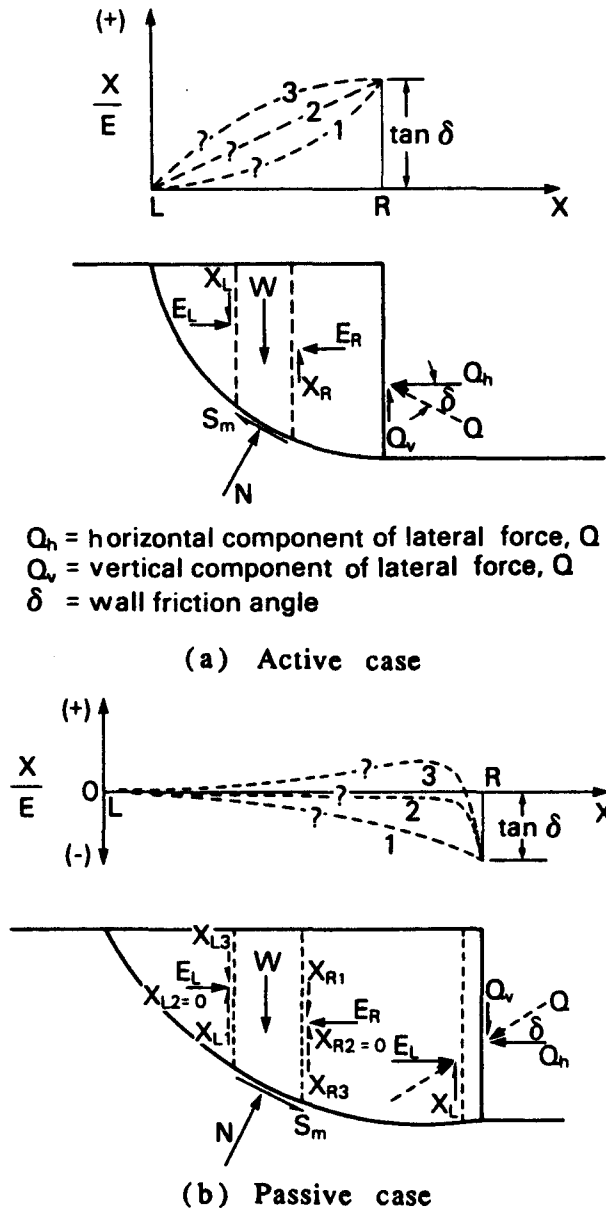

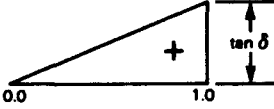
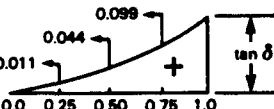
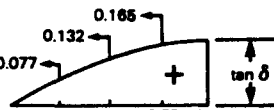


Fig. 2 Assumed interslice force functions for active and passive cases

Some studies of the effect of interslice force functions on the lateral earth force computations have been performed by Rahardjo (1982). Table 1 presents the different interslice force functions used for the active case. The difference in the coefficients of active lateral earth force,  $K_a$ , obtained from different functions is small. However, this is

not true for the passive case. Table 2 shows that different interslice force functions used in the passive case produce significant differences in the coefficients of passive lateral earth force,  $K_p$ . Therefore, the shape of the interslice force function has a greater effect for the passive case than for the active case.

Table 1 Possible interslice force function for active case (unit weight,  $\gamma = 20 \text{ kN/m}^3$ , angle of internal friction,  $\phi' = 30^\circ$ , wall friction angle,  $\delta = -10^\circ$ , height of wall,  $H = 30.0 \text{ m}$ )

No	Interslice function, $X/E$	$Q_{\text{active}}$ (kN)	$K_a = \frac{Q_a}{\frac{1}{2}\gamma H^2}$
1		2790	0.310
2		2776	0.308
3		2779	0.309
4		2773	0.308

( $\tan \delta = 0.176$ )

In general, the magnitude of the lateral earth force decreases as the interslice force function used increases towards a positive value (i.e., the left shear interslice force has a downward direction). For example, the interslice force function No. 3 in Fig. 2b results in lower passive resistance than the zero interslice function when used in the computation of  $K_p$ . The computed passive force is quite sensitive to the assumption made and thus the reasonableness of function No. 3 (Fig. 2b) needs further investigation.

The selection of an interslice force function can also lead to an unreasonable distribution in the normal force at the base of a slice. Figure 3 compares two distributions of normal force (in the passive case) resulting from two interslice force functions. A zero interslice force function (Fig. 3a) assumes no interslice shear force developed along the slice boundary. This means that the vertical component of the lateral earth force is balanced only by the normal force of the last

slice. The result gives an enormously large normal force at the last slice compared with the normal forces acting on the other slices.

An unreasonable normal force distribution can be avoided by using an interslice function which continuously distributes the shear force within the soil mass (Fig. 3b). This type of function produces a continuous distribution of normal force along the slip surface. Therefore, precautions should be exercised in choosing an appropriate interslice force function, especially for the passive case.

Table 2 Possible interslice force functions for passive case (unit weight,  $\gamma = 20 \text{ kN/m}^3$ , angle of internal friction,  $\phi' = 30^\circ$ , wall friction angle,  $\delta = +10^\circ$ , height of wall,  $H = 30.0 \text{ m}$ )

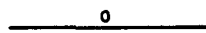
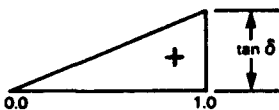
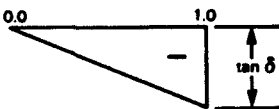
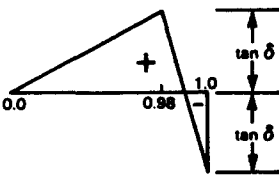
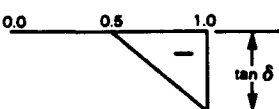
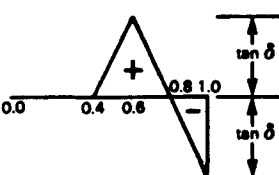
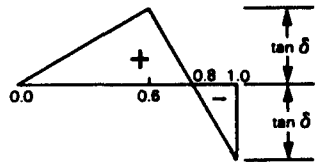
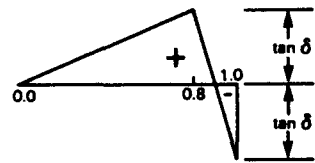
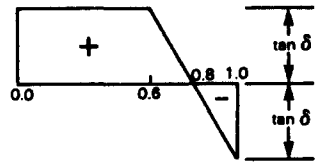
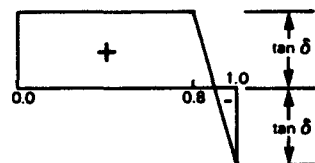
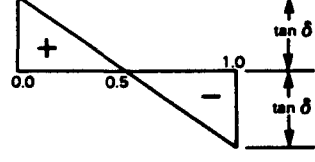
No	Interslice function, X/E	$Q_{\text{passive}}$ (kN)	$K_p = \frac{Q_p}{\frac{1}{2}\gamma H^2}$
1		35557	3.951
2		32924	3.658
3		38912	4.324
4		32885	3.654
5		37226	4.141
6		35125	3.913
(tan $\delta = 0.176$ )			

Table 2 Possible interslice force functions for passive case (unit weight,  $\gamma = 20 \text{ kN/m}^3$ , angle of internal friction,  $\phi' = 30^\circ$ , wall friction angle,  $\delta = +10^\circ$ , height of wall,  $H = 30.0 \text{ m}$ ) (continued)

No	Interslice function, X/E	$Q_{\text{passive}}$ (kN)	$K_p = \frac{Q_p}{\frac{1}{2}\gamma H^2}$
7		34177	3.797
8		33470	3.719
9		34295	3.811
10		33327	3.703
11		36880	4.098
(tan $\delta = 0.176$ )			

### GENERALIZED INTERSLICE FUNCTIONS BASED ON FINITE ELEMENT ANALYSIS

A better understanding of the interslice force function can be obtained through use of a theoretical stress analyses of the soil mass (Morgenstern and Price, 1965). A generalized interslice force function based on finite element stress analyses has been performed by Fan, Fredlund and Wilson (1986) for slope stability problems. The function was formulated on the assumption that the primary factors involved are the geometry of the slope and the force due to gravity. It was assumed that differing moduli of elasticity and Poisson's ratio are of secondary relevance and, therefore, do not significantly affect the shape of the

interslice force function,  $f(x)$ . It was also assumed that it was not necessary to subdivide the interslice normal force into effective and pore-water components.

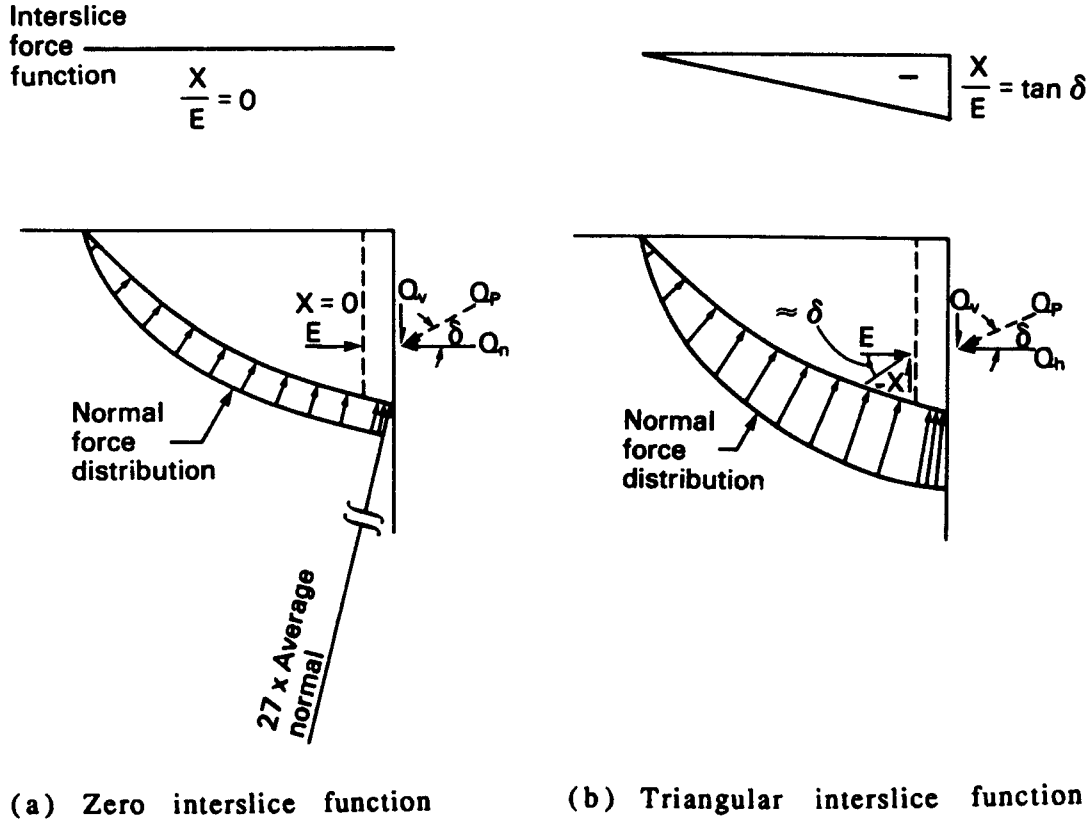


Fig. 3 Effect of the interslice force function on the normal force distribution (passive case)

A two-dimensional, finite element computer program that used constant strain, triangular elements was used to compute the internal stresses in a soil mass. The elements were arranged in a symmetrical manner, which would provide ease in integrating along vertical surfaces. The finite element analysis was performed with the gravity force applied, and the stresses on all elements were computed. Various slip surfaces were then selected and the interslice force function was computed for each slip surface.

The forces of interest are the interslice normal and shear forces (i.e.,  $E$  and  $X$ ). The interslice forces were computed using Simpson's method of integration for the horizontal normal and shear stresses over the vertical sides of each slice (Fig. 4).

The generalized interslice force function, as deduced from numerous finite element analyses has the form of an extended error function:

$$f(x) = Ke^{(-c^n \omega^n)/2} \quad [2]$$



where:

$K$  = the magnitude of the interslice force function at mid-slope (i.e., maximum value)

$c$  = a variable defining the inflection points near the crest and toe of a simple slope

$n$  = a variable specifying the flatness or sharpness of curvature of the function

$\omega$  = the dimensionless position relative to the midpoint of each slope

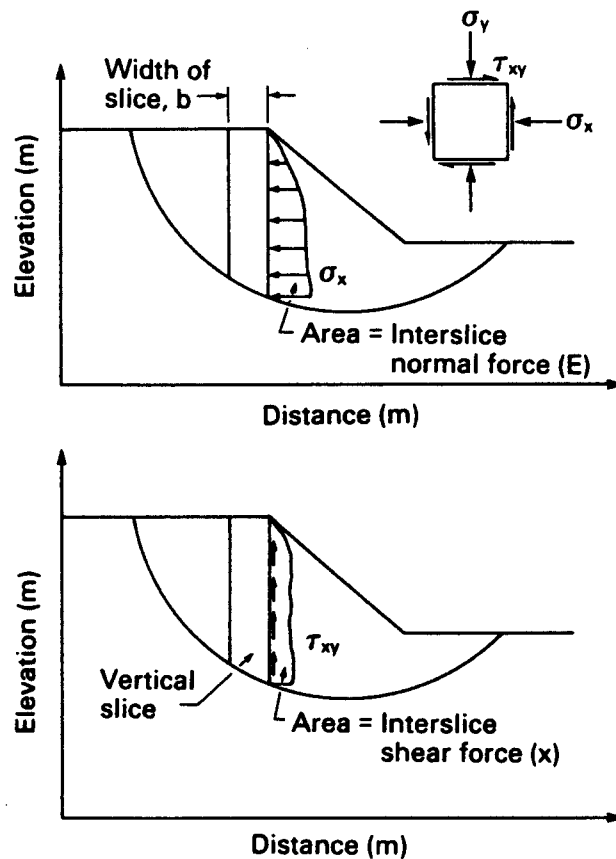
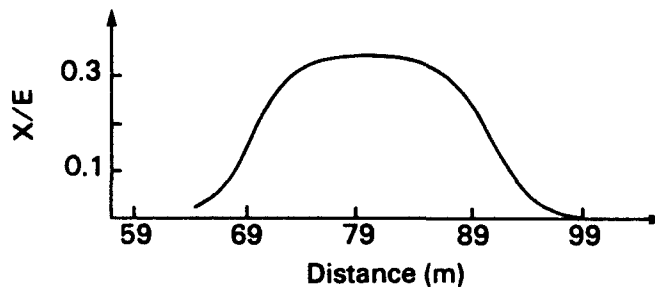


Fig. 4 The normal and shear forces acting on the right side of a slice

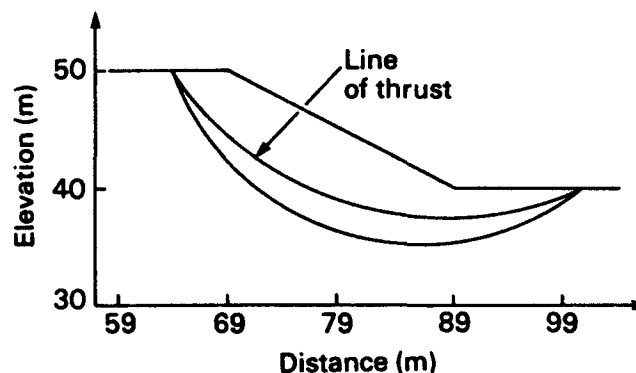
The maximum value of the interslice force function,  $K$ , varies with the slope inclination and the depth of the slip surface as referenced to the height of the slope. The magnitudes of the variables,  $\omega$ ,  $c$  and  $n$ , are functions of the slope inclination. The dimensionless position,  $\omega$ , is measured from the midpoint of the slope in either direction.

Figures 5 and 6 illustrate the interslice force functions generated from Eq. 2 for gentle and steep slopes, respectively. The generated functions are bell-shaped with the peak occurring approximately at

midslope. The resulting line of thrusts, as computed from limit equilibrium analyses, appear to fall within the sliding mass (Figs. 5b and 6b). This is an indication of a physically acceptable solution. Furthermore, the use of the interslice force function in Eq. 2 has been found to be useful in minimizing problems associated with nonconvergent, slope stability solutions.



(a) Interslice force function



(b) Resulting line of thrust

Fig. 5 Interslice force function for a deep-seated slip surface in a 2:1 slope

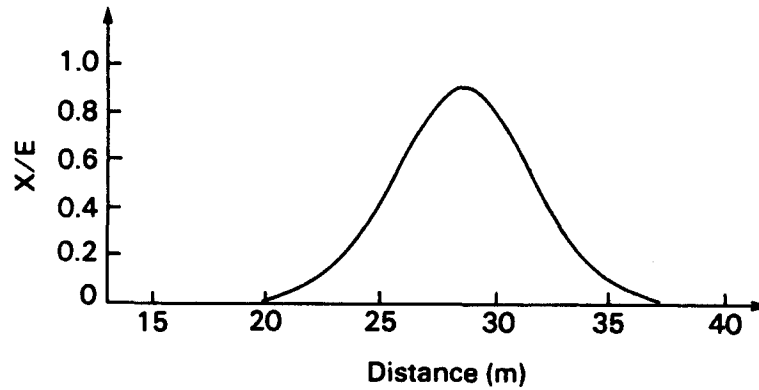
#### GENERATED INTERSLICE FUNCTIONS FOR LATERAL EARTH FORCE

Finite element analyses similar to the ones performed for the slope stability problem (Fig. 4) have also been conducted for lateral earth force problems. Vertical slopes were considered and forces were specified on the nodes along the face of the slope in order to simulate active or passive lateral earth forces. The horizontal forces were calculated in accordance with the Rankine earth pressure theory. The vertical forces were computed as a fraction of the corresponding horizontal forces at the nodes in accordance with the wall friction angle,  $\delta$ .

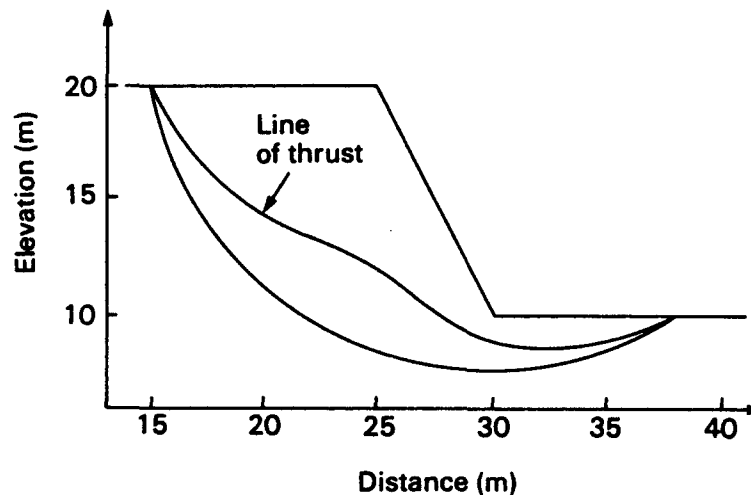
#### Active Case

A typical interslice force function for the active case is shown in Fig. 7. The  $X/E$  ratio is smallest at the beginning of the slip surface. It increases gradually towards the excavation, reaching a peak at the wall. In the upslope region where the slip surface intercepts the horizontal

ground, the soil is almost in an at-rest condition. This implies that the major and the minor principal planes for these soil elements are nearly horizontal and vertical in position. Consequently, the shear stresses produced are small leading to low interslice force ratios in this region.



(a) Interslice force function



(b) Resulting line of thrust

Fig. 6 Interslice force function for a deep-seated slip surface in a 1:2 slope

In the active case, the soil mass tends to slide down due to its own weight. The shearing resistance acts in a direction opposite to the movement of the soil. The displacement of the soil mass mobilizes positive shear stresses for all the elements within the slip surface (i.e., shear stresses which cause a counter-clockwise moment). This phenomenon accounts for positive interslice force ratios across the entire slope.

The peak  $X/E$  ratio for the active case occurs at the wall and this condition can be justified as follows: i) the abrupt change of geometry at the excavation dominates the stress distribution inducing high shear stresses at the vicinity of the wall; ii) the deformation of the soil mass is

largest at the wall and; iii) the mobilization of friction at the interface between the soil and the wall.

Once there is a shear stress developed at the wall, the major and minor principal planes will no longer be horizontal and vertical. Instead, the planes are inclined at an angle which explains the formation of a curved slip surface. Figure 8 shows the interslice force function and the orientations of the principal planes for the active case. The corresponding Mohr-circles illustrate the rotations of the principal planes at the beginning and the end of the slip surface.

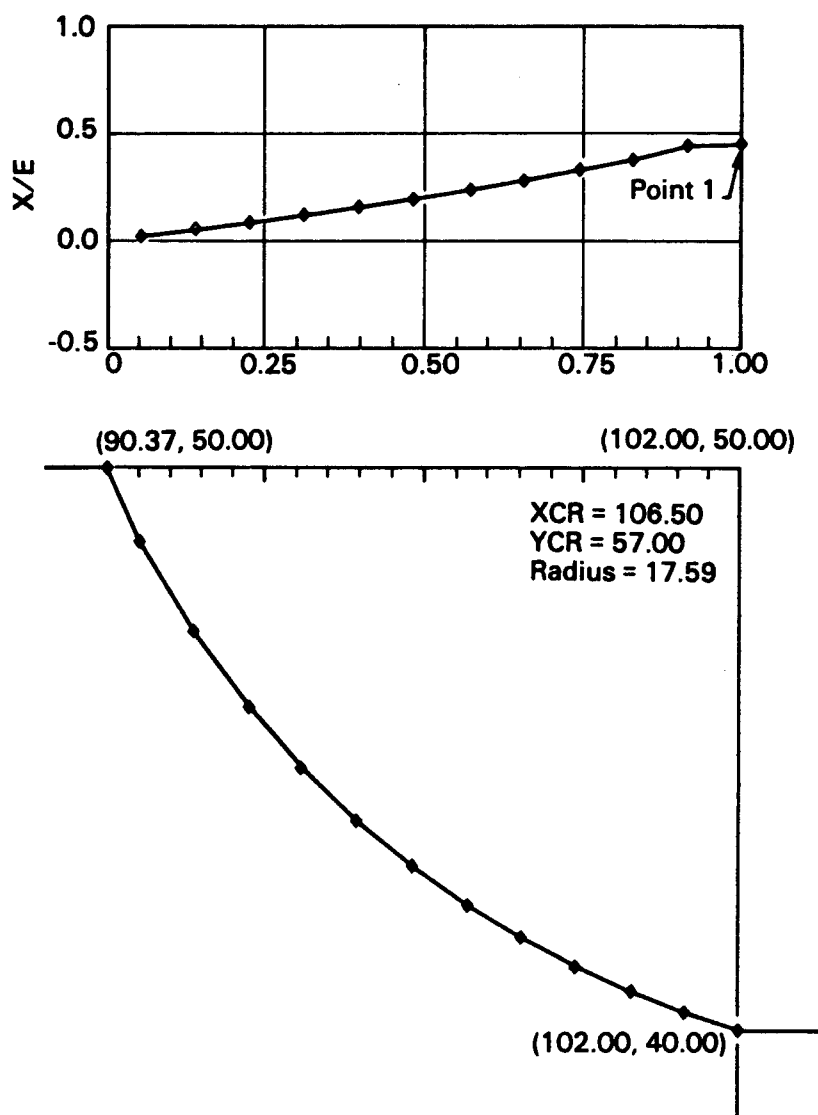


Fig. 7 The interslice side force ratio distribution for the active case ( $\phi = 30^\circ$ ;  $\delta = 15^\circ$ )

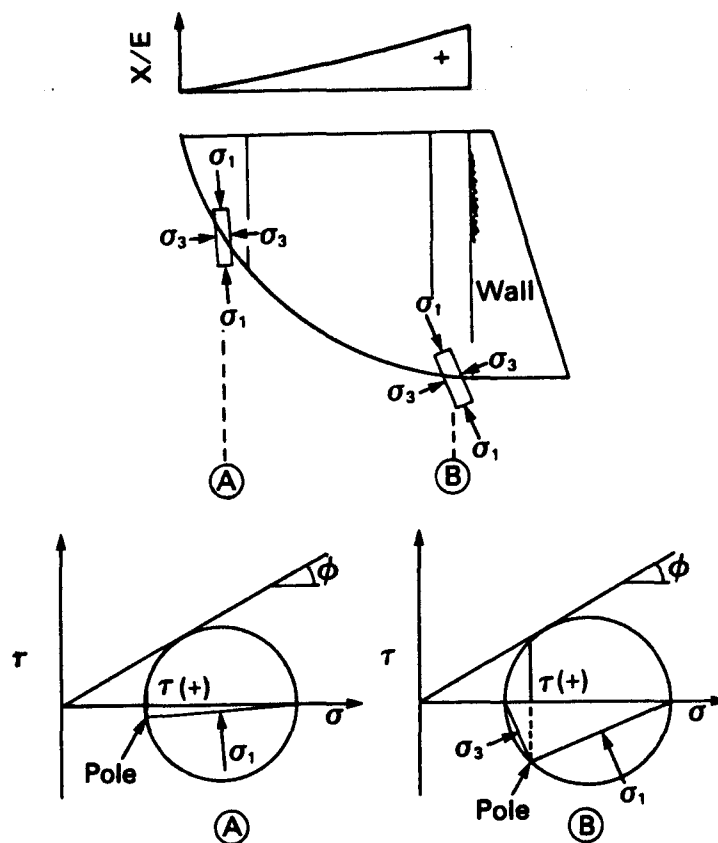


Fig. 8 The interslice force function and the orientations of the principal planes for the active case

### Passive Case

A typical interslice force function for the passive case is illustrated in Fig. 9. In the passive case, the shear force mobilized along the slip surface acts downward since the soil mass is being pushed upward by the external forces. The interslice side force ratio is most negative at the wall due to the presence of high shear stresses. The shear stresses occur as a result of soil displacement as well as the mobilization of wall friction. The magnitude of the side force ratio dissipates from a maximum at the wall to zero at some distance from the excavation. To the left of the point where the shear force vanishes, the interslice side force ratios can be either positive or remain close to zero depending on the geometry of the slip surface and the shear strength parameters of the soil. The latter is generally found to be true for the more critical cases. The low interslice force ratios in this region can be accounted for by the extremely small interslice shear forces compared to the interslice normal forces. This implies that the major and minor principal planes are almost horizontal and vertical in direction.

For the critical passive case, the slip surface in the up-slope region is nearly planar in shape. For limit equilibrium computations

involving a planar slip surface, the result is found to be independent of the interslice force function (Rahardjo, 1982). Therefore, the shape of the function at the up-slope region is not critical to the final result as long as the slip surface is approximately planar. The interslice side force ratios in this region were found to be close to zero. Figure 10 shows the interslice force function and the orientations of the principal planes for the passive case. A Mohr circle is drawn to illustrate the direction of the principal planes at the beginning and the end of the slip surface.

### APPLICATION OF THE GENERALIZED FUNCTION TO THE LATERAL EARTH FORCE PROBLEMS

The same generalized function which models the interslice force function for the slope stability problems (Eq. 2) can also be used in predicting the interslice force functions for lateral earth force problems. In order to use this function for the active case, it is necessary to obtain the maximum interslice side force ratio at the wall (i.e., point 1 in Fig. 7). This point can be determined from a mathematical equation which relates the maximum X/E ratio to the wall

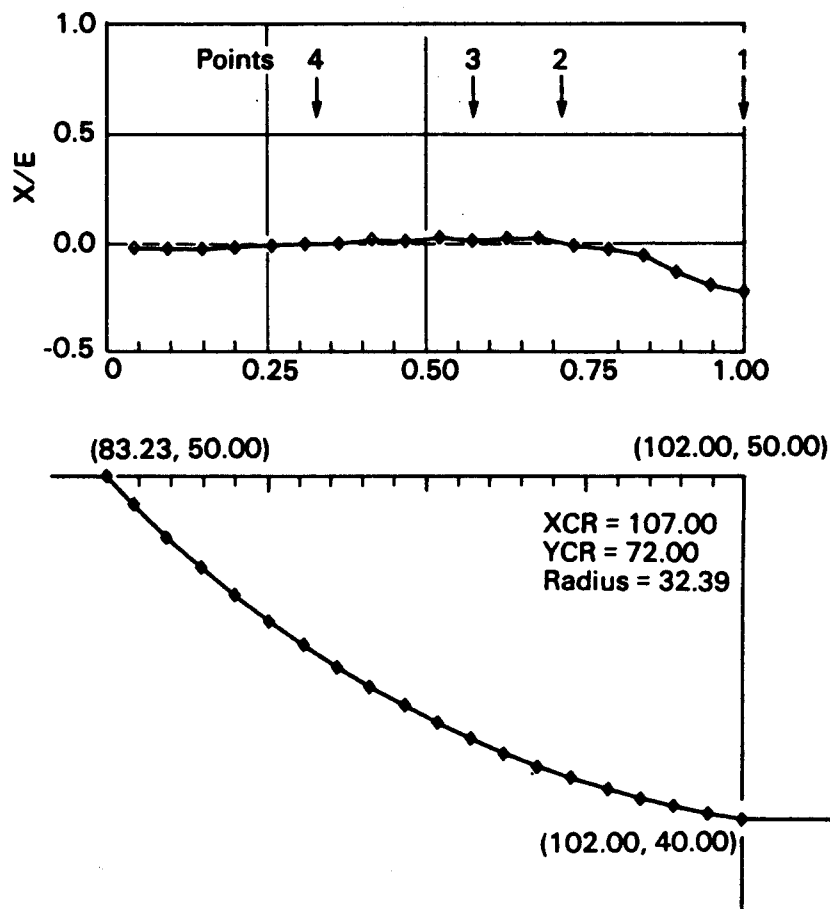


Fig. 9 The interslice side force ratio distribution for the passive case ( $\phi = 20^\circ$ ;  $\delta = 20^\circ$ )

and soil friction angles (Fan, 1983). The predicted function from Eq. 2 is almost identical to the functions generated from the finite element analyses as illustrated in Fig. 11 for a typical active case.

For the passive case, four points on the generated function from finite element analyses are used as reference points (i.e., points 1, 2, 3 and 4 in Fig. 9). Points 1 and 2 are a function of the soil and wall friction angles. On the other hand, points 3 and 4 are a function of the height of the slope and the distance of these points from the intersection point of the slip surface to the ground surface (Fan, 1983). These four points can be joined by a series of straight lines. The interslice side force ratio,  $X/E$ , at any point along the horizontal axis can be interpolated using these four points. The straight line approximation method appears to serve reasonably well in predicting the interslice force function for the passive case as illustrated in Fig. 12.

The generalized functions for the active and passive cases have also been studied using the problems presented in Tables 1 and 2, respectively. The use of the generalized function for the active case resulted in a computed  $Q_{active}$  of 2754 kN and the computed  $K_A$  of 0.306. These are in close agreement with the results obtained from other

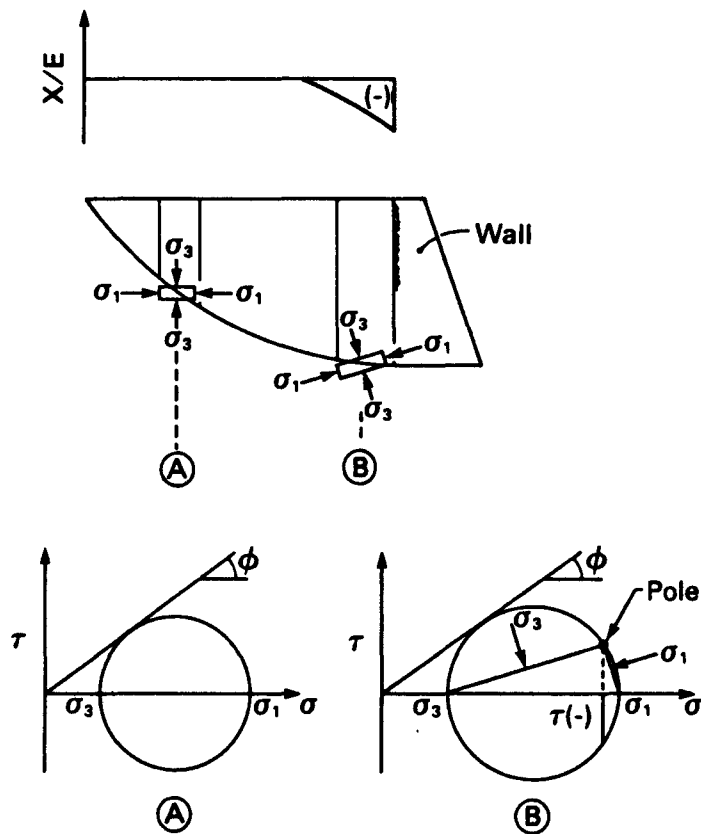


Fig. 10 The interslice force function and the orientations of the principal planes for the passive case.

functions in Table 1. This confirms the insensitivity of the active lateral earth force with respect to the use of various interslice force functions. On the other hand, the generalized function for the passive case gave  $Q_{\text{passive}}$  of 36,274 kN and  $K_p$  of 4.030. Although these values agree closely with the results obtained from zero interslice force function (i.e., function No. 1 in Table 2), the generalized function results in a more reasonable distribution of normal forces along the slip surface (e.g., see Fig. 3).

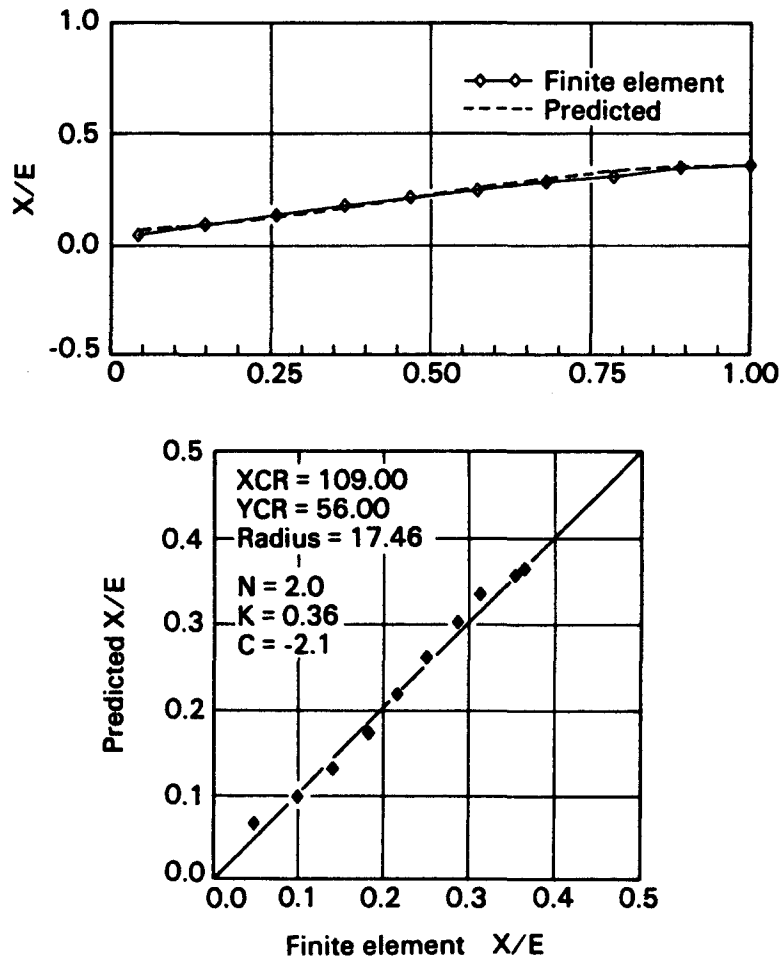


Fig. 11 X/E computed by the generalized function (predicted) versus X/E computed by the finite element method in the active case



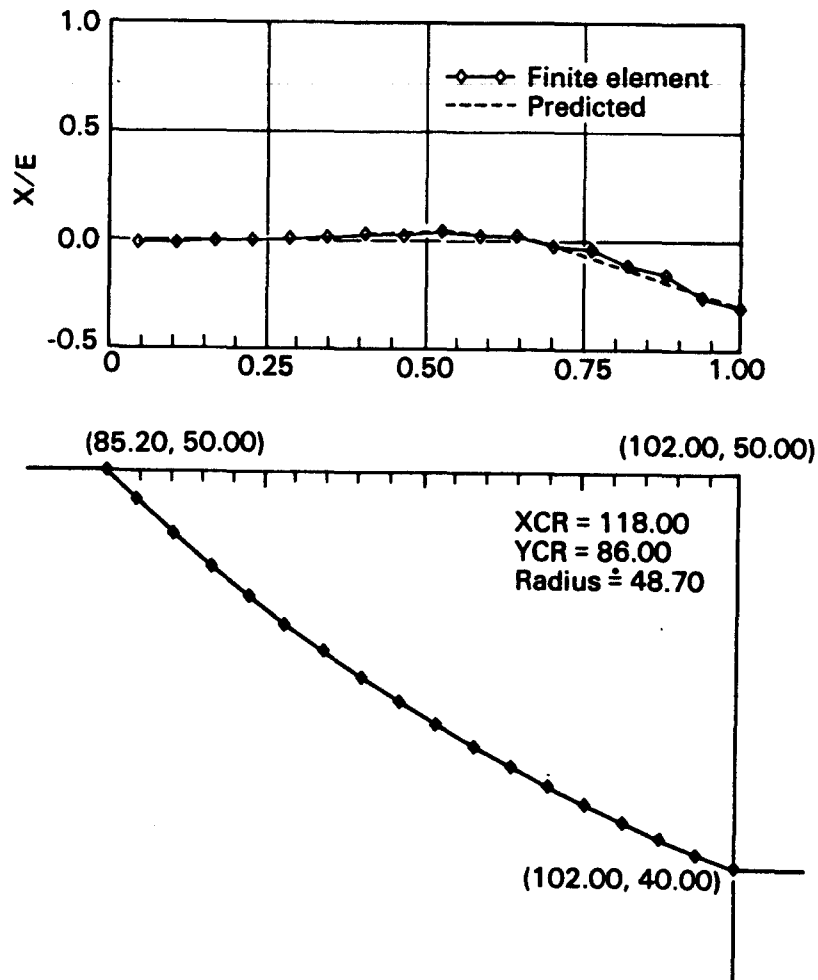


Fig. 12 X/E computed by the straight line approximation method (predicted) versus X/E computed by the finite element method in the passive case

### CONCLUSIONS

The following conclusions can be drawn from this paper:

1. The interslice force functions for simple homogeneous slopes with circular-slip surfaces are bell-shaped and mathematically bear the form of an extended error function.
2. The interslice force function for the active earth pressure case is essentially triangular in shape. It increases gradually to a peak value at the wall where the shear force mobilized is a maximum.
3. The interslice force function for the passive earth pressure case is negative at the wall. This negative shear stress dissipates and eventually vanishes at some distance from the wall. From this point, the ratios remain close to zero. The selection of an appropriate interslice force function is essential for an accurate passive earth pressure analysis.

## **ACKNOWLEDGEMENT**

The authors would like to thank Mr. Zai Ming Zhang of the Beijing Geotechnical Institute for his assistance on the preparation of this research paper.

## **REFERENCES**

- Bishop, A.W. (1955) "The Use of the Slip Circle in the Stability Analysis of Slopes", *Geotechnique*, Vol. 5, 7-17.
- Fan, K. (1983) "Evaluation of Interslice Forces for Lateral Earth Force and Slope Stability Problems", M.Sc. Thesis, University of Saskatchewan, Saskatoon, Saskatchewan.
- Fan, K., Fredlund, D.G. and Wilson, G.W. (1986) "An Interslice Force Function for Limit Equilibrium Slope Stability Analysis", *Can. Geotech. J.*, 23, 287-296.
- Fredlund, D.G., Krahn, J. and Pufahl, D.E. (1981) "The Relationship between Limit Equilibrium Slope Stability Methods", *Proc. of the 10th Int. Conf. on Soil Mech. and Foundation Engrg.*, Stockholm.
- Janbu, N. (1957) "Earth Pressure and Bearing Capacity Calculations by Generalized Procedure of Slices", *Proc. of the 4th Int. Conf. on Soil Mech. and Foundation Engrg.*, 2, 207-212.
- Morgenstern, N.R. and Price, V.E. (1965) "The Analysis of the Stability of General Slip Surface", *Geotechnique*, Vol. 15, 79-93.
- Morgenstern, N.R. and Eisenstein, Z. (1970) "Methods of Estimating Lateral Loads and Deformations", 1970 Specialty Conf. on Lateral Stresses in the Ground and Design of Earth Retaining Structure, A.S.C.E., New York, 51-102.
- Rahardjo, H. (1982) "Lateral Earth Force Calculations Using Limit Equilibrium", M.Sc. Thesis, University of Saskatchewan, Saskatoon, Saskatchewan.
- Rowe, P.W. (1963) "Stress-Dilatancy, Earth Pressures and Slopes", *Journal of the Soil Mechanics and Foundations Division, A.S.C.E.*, Vol. 89, No. SM3, 37-61.